Supporting information

for

Effect of Sb and Na incorporation in Cu_2ZnSnS_4 solar cells

Md Abdul Aziz Suzon[a,b], Louis Grenet[a,b,*], Fabrice Emieux[a,b], E. de Vito[a,b], Frédéric Roux[a,b], Henri Mariette[a,c]

[a] Univ. Grenoble Alpes, F-38000 Grenoble, France

[b] CEA, LITEN, 17, rue des Martyrs, F-38054, Cédex 09 Grenoble, France

[c] CNRS, Institut Néel, 25, rue des Martyrs, F-38042, Grenoble, France

[*] Corresponding author: louis.grenet@cea.fr

In the present study, we aim at demonstrating the role of Na and Sb on the photovoltaic properties of CZTS-based solar cells. However, it is already demonstrated that the cationic composition of the absorber has a strong impact on the device properties [18]. Thus, a carreful attention has been paid to measuring the stoichiometry of the samples used in this study. The list of the sample along with their Cu, Zn and Sn contents (Cu/Zn+Sn, Zn/Sn, Cu/Sn and Cu/Zn ratio are given in the sake of comparison with oher studies) measured by EDS is given in Table S1. Some small random variations can be found between all samples but which cannot explain the regular variation observed in the study.

Table S1: List of the samples used in this study with their cationic composition measured by EDS.

Sample	Cu(%)	Zn(%)	Sn(%)	Cu/Zn+Sn	Zn/Sn	Cu/Sn	Cu/Zn
Undoped	42.4	30.7	26.9	0.74	1.14	1.57	1.38
PAS(Sb5)	42.7	30.1	27.2	0.75	1.11	1.57	1.42
PAS(Sb10)	42.3	30.6	27.1	0.73	1.13	1.56	1.38
PAS(Sb20)	43.0	30.3	26.6	0.76	1.14	1.62	1.42
PAS(Na10)	43.1	29.3	27.6	0.76	1.06	1.56	1.47
PAS(Na15)	43.0	29.9	27.0	0.76	1.11	1.59	1.44
PAS(Na20)	42.8	30.3	26.9	0.75	1.13	1.59	1.41
PAS(Na40)	43.2	29.5	27.2	0.76	1.09	1.59	1.46
PDT(Na10)	42.0	31.3	26.7	0.72	1.17	1.57	1.34
PDT(Na20)	42.9	30.2	26.9	0.75	1.12	1.59	1.42
PDT(Na40)	42.5	30.6	26.8	0.74	1.14	1.59	1.39
PDT(Na60)	42.2	30.4	27.3	0.73	1.11	1.55	1.39
PAS(Na10+Sb10)	42.8	29.4	27.8	0.75	1.06	1.54	1.45

The process described in this study has been optimized by using a high sulfur source temperature (230°C) to achieve a solar cell with 5.9% power conversion efficiency. J-V curves and EQE spectrum of the record cell are shown in Fig. S1(a) and S1(b) respectively. Compared to the state-of-the-art device [8], our record cell exhibit a larger V_{OC} (776 mV against 731 mV) but suffers from lower J_{SC} (13.5 mA.cm^{-2} against 21.7 mA.cm^{-2}), partly because of the lack of anti-reflecting coating in our case.

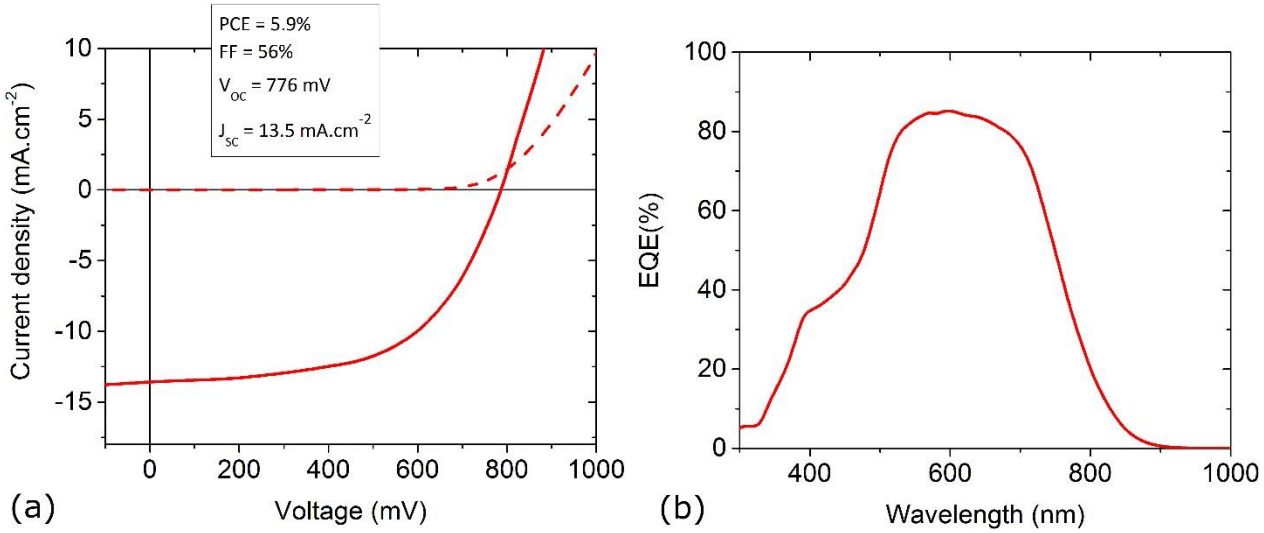

Figure S1: (a) J-V characteristics of the best Mo/CZTS/CdS/i-ZnO/ZnO:Al solar cell along with its PV properties. (b) EQE of the same device.

ToF-SIMS has been used (Fig. 1) to demonstrate the incorporation and the location of Na and Sb in kesterite absorbers. In order to facilitate the comparison of the different Na profiles, the ToF-SIMS signal has been integrated close to the surface (0 nm – 100 nm depth), in the bulk of the absorber (100 nm – 1500 nm depth) and in the Mo. These result are presented in Fig. S2(a).

As NaF is used as Na source in all the experiments, the F profiles have been determined as well with ToF-SIMS and are depicted in Fig. S2(b). The increase in F amount in the absorber (bulk and interface) and in Mo compared to the undoped sample is significant and thus the influence of F on PV properties should be studied as well. However, it is out of the scope of this study.

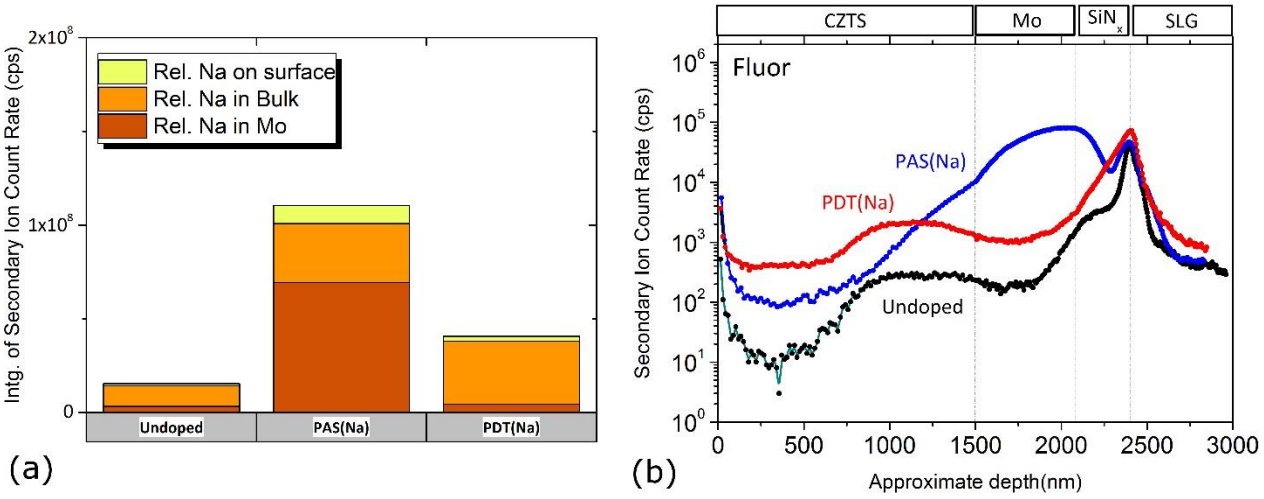

Figure S2 : (a) Integration of the Na signal measured by ToF-SIMS (Fig. 1(a)) for the undoped, PAS(Na) and PDT(Na) samples at the front surface, in the absorber bulk and in Mo. (b) F (Fluor) ToF-SIMS profiles in CZTS/Mo/SiN_x/SLG structures

To understand the modification of the absorber morphology with Na and Sb addition, XRD scans have been performed and are depicted in Fig. S3. These θ-2θ scans are centered on the (112) and (220,204) peaks of the CZTS absorber at 28.5° and 47.3° respectively (PDF 04-017-3032). The (110) Mo peak at

about 40° is used as a reference. $I_{112}/I_{220,204}$ preferential orientation of the layers (Fig. 3) is assessed by measuring the ratio of the area underneath each peak.

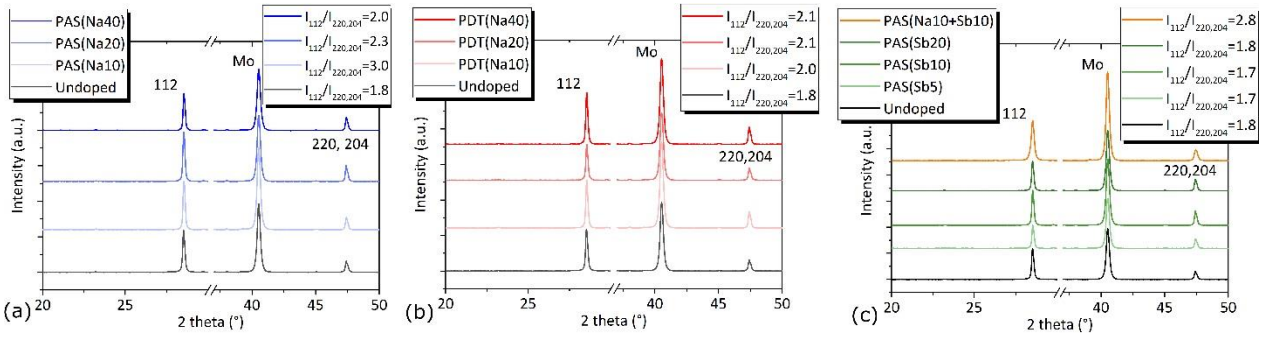

Figure S3: XRD patterns of the (a) PAS(Na), (b) PDT(Na) and (C) PAS(Sb) and PAS(Na+Sb) samples.

To elucidate the origin of PV properties improvement with Na addition in CZTS absorber, EQE spectra and C-V measurements have been performed on all these samples and are depicted in Fig. S4. On the EQE spectra, the current gain compared to the undoped sample is clearly visible both at short wavelengths (below 600 nm) and at long wavelengths (above 600 nm). This higher quantum efficiency has been attributed in the first case to reduced interface recombination [21] and to longer collection length in the second case [21]. By simple data manipulation and strong assumptions on the device model [22], it is possible to extract both the majority carrier density $N_{C\text{-}V}$ and the depletion width W in the absorber.

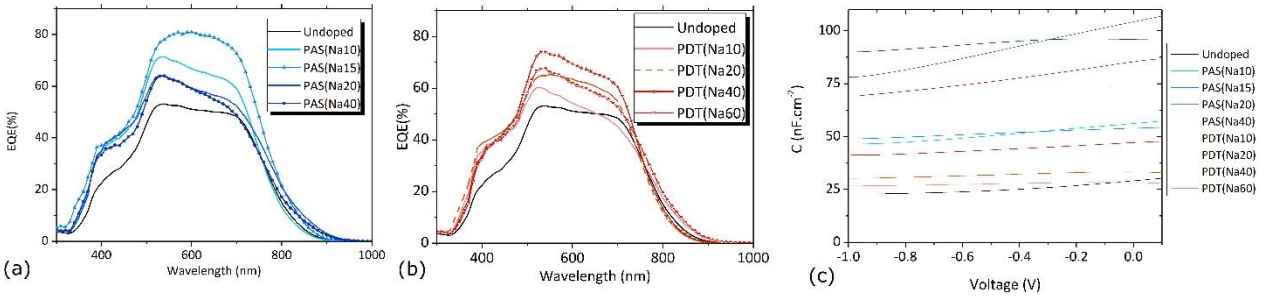

Figure S4: EQE spectra of the (a) PAS(Na) and (b) PDT(Na) samples. (c) Capacitance-voltage curves of all samples measured at room temperature.

In order to have a better quantification of the contribution of the bulk and interface losses reduction with Na addition, all EQE spectra have been fitted with e-ARC simulation software [20]. Results of the simulations are depicted in Fig. S5. On this graph, and for all samples, the simulated EQE spectrum is depicted in red line and compared with the experimental one in black circles. Two parameters are adjusted to obtain the best fit: the carrier collection length L_C and the thickness of the dead layer Th_d located at the CZTS/CdS interface. This layer is used in e-ARC to account for the interface recombination: the dead layer has got the same optical properties as the absorber but carriers generated within the dead layer do not contribute to the collected current [20]. Thus, the light absorbed in this layer is lost, which accounts for the interface recombination: the thicker the dead layer, the higher the interface recombination rate.

The e-ARC software automatically calculates the current (electron-hole pairs) generated in each layer (colored area on Fig. S5), including the dead area in green and gives as a result the current lost in the different regions of the device (back contact, front contact, interface (dead area) and bulk due to the insufficient collection). The small discrepancy between simulated and experimental EQE at very long

wavelengths is attributed to back interface recombination (which has not been taken into account with a dead layer at the back interface).

By combining C-V measurements and EQE simulation, it is possible to assess the minority carrier diffusion length L_D in the absorber ($L_C = L_D + W$) [20].

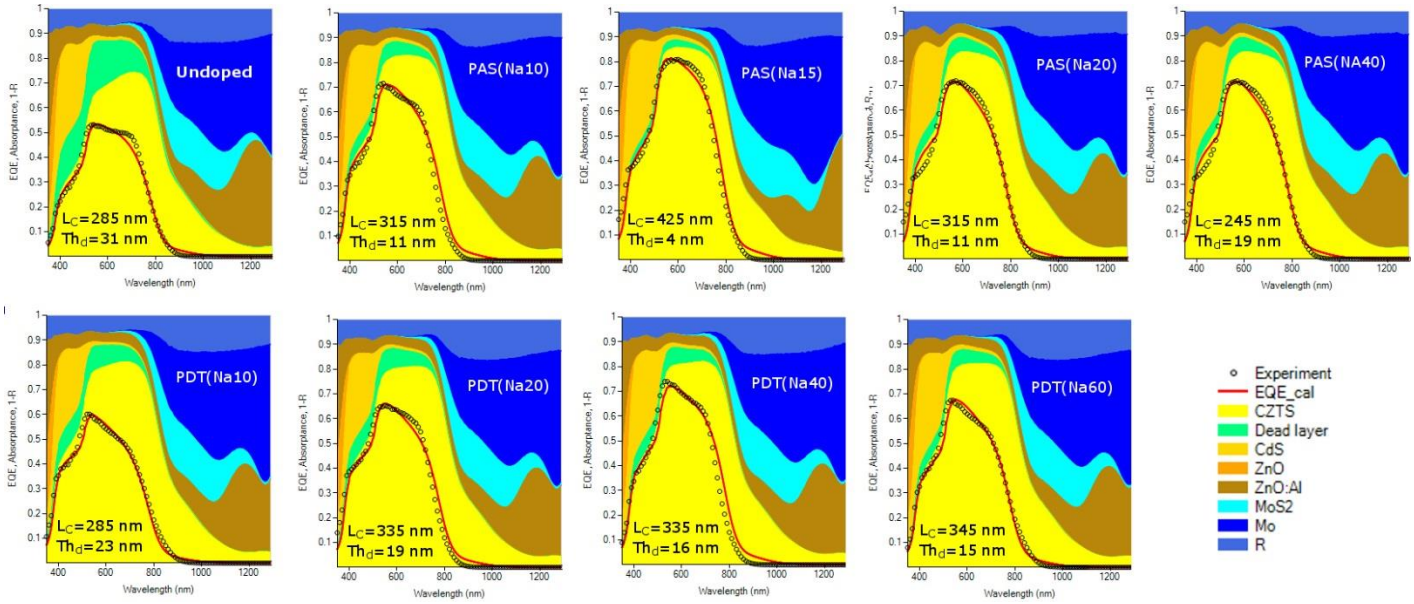

Figure S5: Simulated EQE spectra (red line) along with experimental EQE spectra (black circle) for all the samples. Carrier collection lengths and thickness of the dead layer found for the best fit are written on each graph.